

Ethylenediamine on Ge(100)-2 × 1: The Role of Interdimer Interactions

Ansoon Kim,[†] Michael A. Filler,[‡] Sehun Kim,[†] and Stacey F. Bent^{*,‡}

Department of Chemistry and School of Molecular Science (BK21), Korea Advanced Institute of Science and Technology, Daejeon 305-701, Republic of Korea, and Department of Chemical Engineering, Stanford University, Stanford, California 94305-5025

Received: August 4, 2005

We have investigated the reaction of the bifunctional molecule ethylenediamine on Ge(100)-2 × 1 using multiple internal reflection Fourier transform infrared spectroscopy, X-ray photoelectron spectroscopy, and density functional theory calculations. Ethylenediamine exhibits different adsorption behavior than simple methylamines on the Ge(100)-2 × 1 surface. At low coverages, ethylenediamine undergoes dissociative chemisorption via an interdimer dual N–H dissociation reaction. As coverage increases, the N–H dissociation reaction is inhibited and formation of a Ge–N dative-bonded structure dominates.

Introduction

Over the past decade, organic functionalization of semiconductor surfaces has emerged as an important growth area in the development of molecule-based devices.^{1–3} The incorporation of organic molecules with specific properties at the semiconductor surface has the potential to impart novel functionalities to various nanoscale devices. A detailed understanding of the chemistry of molecule–semiconductor surface systems is required to determine the fundamental and technological challenges of developing new surface-modified semiconductor devices.

The potential to create versatile multilayer structures and films drives interest in the attachment of bifunctional molecules at the semiconductor surface. On a properly engineered bifunctional molecule, one moiety reacts with the surface, acting as an attachment point, while the remaining functional group points away from the surface and is thus available for subsequent layer attachment. A sequential “molecular layer deposition” process utilizing bifunctional compounds can then enable the creation of ultrathin organic films.^{4–6}

Recent studies have demonstrated that analogies between the organic functionalization of (100)-2 × 1 group IV semiconductor surfaces and classic solution-phase organic chemistry provide a method of characterizing and understanding these surface reactions.^{7–10} The reconstructed Si(100)-2 × 1 and Ge(100)-2 × 1 surfaces consist of dimers that are connected by a strong σ -bond and a weak π -bond. The partially π -bonded surface dimers tilt out of the surface plane, and this distortion induces a charge transfer from the “down” (electrophilic) to the “up” (nucleophilic) surface atom.¹¹ Such zwitterionic character allows the surface to undergo nucleophilic/electrophilic reactions, often with direct analogies to molecular systems.¹⁰

On Si(100)-2 × 1 and Ge(100)-2 × 1, dative bonding, also known as coordinate covalent bonding, involves charge donation either from the lone pair of an impinging molecule to the electrophilic dimer atom of the surface or from the nucleophilic dimer atom to an electron-deficient orbital of an impinging

molecule.¹⁰ Previous investigations of the adsorption of compounds with at least one lone pair of electrons on Si(100)-2 × 1 and Ge(100)-2 × 1 reveal that dative bonds exist as stable surface adsorbates and also as precursor states to subsequent surface reaction.¹⁰ Methylamines, which contain an sp^3 hybridized nitrogen atom with a lone pair of electrons and are thus similar to ethylenediamine, have been extensively studied by several research groups.^{12–18} Of particular significance is a study on Ge(100)-2 × 1 by Mui et al. which concluded that monomethyl-, dimethyl-, and trimethylamine all form a Ge–N dative bond at room temperature.¹⁵

In the present work, we investigate the reaction of the bifunctional molecule ethylenediamine on Ge(100)-2 × 1 using multiple internal reflection Fourier transform infrared (MIR-FTIR) spectroscopy, X-ray photoelectron spectroscopy (XPS), and density functional theory (DFT). Figure 1 illustrates several probable reaction pathways of ethylenediamine on Ge(100)-2 × 1. It is important to note that these pathways involve both single and multiple surface dimers in intra- and interdimer bonding configurations, respectively. Ethylenediamine may form a dative bond between the lone pair of one of its amine groups and the electrophilic dimer atom of a single surface dimer (Figure 1a). Following adsorption in the dative-bonded state, subsequent N–H dissociation via proton transfer is also possible, although we will show that this intradimer pathway is not energetically favorable. The bifunctional nature of ethylenediamine also provides the possibility of interdimer interactions, displayed in Figure 1b, where each amine group bonds to adjacent surface dimers. The interdimer reaction can lead to a dual dative bond or to a N–H dissociation in one or both amine groups. Similar types of interdimer interactions have been previously reported for the adsorption of nitriles,¹⁹ unsaturated ketones,²⁰ carboxylic acids,²¹ cyclic dienes,²² and ethylene²³ on Si(100)-2 × 1 and Ge(100)-2 × 1.

We will show that ethylenediamine undergoes two distinct reactions on Ge(100)-2 × 1 at low and high surface coverage. At low coverage, a dual N–H dissociation occurs wherein both amine groups react at adjacent dimer sites, while at higher coverages, a dative-bonded product dominates.

* To whom correspondence should be addressed. E-mail: sbent@stanford.edu.

[†] Korea Advanced Institute of Science and Technology.

[‡] Stanford University.

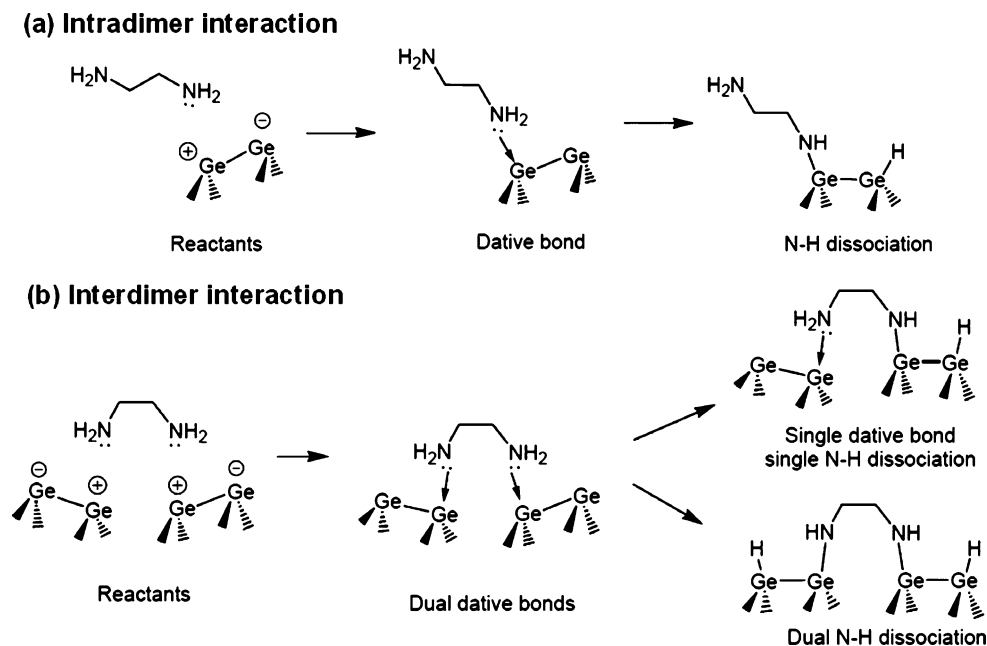


Figure 1. Possible (a) intradimer and (b) interdimer surface reaction products of ethylenediamine on the Ge(100)- 2×1 surface.

Experimental and Computational Details

IR experiments were completed under ultrahigh vacuum conditions (UHV) in a reaction chamber described previously.¹⁵ The base pressure in the chamber is less than 1×10^{-10} Torr. Unpolarized spectra were collected by employing a Fourier transform infrared (FTIR) spectrometer equipped with a narrow-band HgCdTe detector with the Ge crystal (19 mm \times 14 mm \times 1 mm, 45° beveled edges) in a multiple internal reflection (MIR) geometry. The crystal was cleaned using Ar⁺ ion sputtering (8–9 μ A, 0.5 kV) at room temperature, followed by annealing to 900 K for 5 min. Although the cleaning procedure in this chamber differed from that in our XPS chamber, after several sputtering/annealing cycles, the LEED pattern of the 2×1 surface reconstruction was clearly visible. Auger electron spectroscopy (AES) verified that carbon, oxygen, and nitrogen surface concentrations were undetectable. A thin tantalum plate covered the back face of the crystal to minimize unwanted adsorption/reaction on the uncleaned side. A background IR emissivity spectrum for the clean crystal was recorded, and subsequent scans after adsorption of ethylenediamine and ethylene-*d*₄ diamine were ratioed to this background and transformed to absorbance spectra. Multilayers were condensed on the surface near 130 K to obtain IR spectra of the unreacted precursors. For each spectrum, at least 1000 scans were averaged at 4 cm⁻¹ resolution and were corrected for baseline sloping.

X-ray photoelectron studies were carried out in a reactor constructed from stainless steel and equipped with a 220 L/s ion and Ti sublimation combination pump (Perkin-Elmer, TNB-X) as well as a 180 L/s turbomolecular pump (Pfeiffer-Balzars, TPU 180H) in the main chamber. This pumping combination achieves an overall chamber base pressure less than 1×10^{-10} Torr as measured by a hot-cathode ionization gauge. The X-ray photoelectron spectrometer consists of a dual anode X-ray source (Specs, XR-50) and a five channeltron hemispherical analyzer (Specs, Phoibos 100). The Ge(100) crystal (approximately 3 mm \times 10 mm) can be heated resistively and cooled by heat exchange with a liquid nitrogen reservoir in contact with the sample holder through a copper braid.

For X-ray photoelectron experiments, the Ge(100) crystal (0.1–0.39 Ω cm, p-type, B-doped) was cleaned by Ar⁺

sputtering at 900 K (20 mA emission current, 1.0 keV accelerating voltage, 12 μ A sample current) for 30 min followed by annealing to 1000 K for 15 min. Following several sputtering/annealing cycles, carbon, oxygen, and nitrogen levels were below the detection limit of our X-ray spectrometer and STM images confirmed a mixed $c(4 \times 2)$ and 2×1 surface reconstruction.²⁴ Due to interference by the germanium Auger series, it was necessary to record C(1s) and N(1s) photoelectron spectra (250 W = 12.5 kV anode voltage, 20 mA emission current) with the Al and Mg anodes, respectively. The emitted electrons were collected at a takeoff angle of 25°, with an acceptance angle of ca. $\pm 5^\circ$, and a pass energy of 25 eV. The Ge(3d) photoelectron peak was employed as an internal standard with which to calibrate the energy scale and peak intensity. Shirley baselines²⁵ were applied, and an experimentally realistic number of Voigt components was fit to each photoelectron spectrum. With our spectrometer set at a pass energy of 25 eV, the C(1s) spectrum of ethylene chemisorbed on Ge(100)- 2×1 shows a single peak centered at 283.7 eV with a fwhm of 1.6 eV. While all synthetic components within each spectrum were forced to have the same fwhm, the value was allowed to range between 1.6 ± 0.2 eV.

Ethylenediamine (Aldrich, 99+%) and ethylene-*d*₄ diamine (Aldrich, 98 atom D %) were transferred to sample vials in a nitrogen-purged glovebox. Both compounds were purified by several freeze–pump–thaw cycles before being introduced into either system. The molecular identities of both compounds were verified after exposure to the crystal with a quadrupole mass spectrometer. Surface exposures were measured in langmuirs (1 L = 10^{-6} Torr·s), and dosing was performed by filling each chamber to a particular pressure for a specified period of time. Pressures were not corrected for ion gauge sensitivity.

Potential energy surface calculations were completed with the Jaguar 5.5 software package using Becke3 Lee–Yang–Parr (B3LYP) three-parameter density functional theory.²⁶ One dimer (Ge₂H₁₂) and two dimer trench (Ge₃₁H₃₂) clusters were used to model both intradimer and interdimer pathways, respectively. The geometries of important local minima on the potential energy surface were determined at the B3LYP/LACVP** level of theory.²⁷ The LACVP** is a mixed basis set, using the

LACVP basis set to describe the Ge atoms and the 6-31G basis set for the remaining atoms. Structures for the one-dimer model were fully optimized without geometrical constraints. To minimize aphysical cluster geometries,²⁸ the positions of the third and fourth layer Ge atoms of the trench clusters were fixed at the experimentally determined positions of the Ge(100)-c(4 × 2) surface reconstruction.²⁹ Local minima and transition states were verified with frequency calculations of the optimized structure, and all reported energies were zero point corrected.

Although similar cluster models have been employed to study the reaction of other amines on Si(100)-2 × 1 and Ge(100)-2 × 1,^{13,15,30–32} a few comments regarding our use of a c(4 × 2) trench cluster to model the surface reactions of ethylenediamine are necessary. While Ge(100) surface preparation procedures often give a combination of c(4 × 2), p(2 × 2), and 2 × 1 reconstructed domains at room temperature,²⁴ several recent scanning tunneling microscopy (STM) studies report that adsorbate and tip-induced surface reconstruction transitions are facile on Ge(100)-2 × 1. Kim and co-workers found c(4 × 2)/2 × 1 to c(4 × 2) and c(4 × 2)/2 × 1 to p(2 × 2) transitions upon the adsorption of the nitrogen-containing compounds pyridine³³ and pyrimidine,³⁴ respectively, on Ge(100)-2 × 1 at room temperature. Low-temperature studies also reveal that moderate applied biases from a STM tip can cause a reversible transition from a c(4 × 2) to p(2 × 2) structure and vice versa on Ge(100)-2 × 1.^{35,36} Furthermore, due to the hybridization of each surface dimer atom, pyrimidine is observed to react with two dimers in adjacent rows,³⁴ suggesting that inter-row bonding is more likely than intra-row bonding. Together these studies provide strong evidence that a cross-trench c(4 × 2) cluster is accurate for modeling the reaction pathways in this work.

Results and Discussion

Coverage-dependent IR spectra of the exposure of ethylenediamine to a clean Ge(100)-2 × 1 surface at room temperature are shown in parts a–c of Figure 2. Figure 2d shows the multilayer spectrum of unreacted ethylenediamine at 130 K. Vibrational mode assignments for each surface product are completed by comparison with the multilayer spectrum as well as various literature sources.^{37,38} Following an exposure of 0.5 L (Figure 2a), a peak corresponding to a $\nu(\text{Ge-H})$ stretch is clearly visible at 1944 cm^{-1} . The presence of this mode indicates that ethylenediamine undergoes either N–H or C–H dissociation. Although the process of hydrogen desorption from the chamber walls and subsequent reaction at the surface to form Ge–H bonds is theoretically possible, we do not observe any Ge–H growth after exposing a clean Ge(100)-2 × 1 surface to vacuum ($p < 10^{-9}$ Torr) for 8 h. In addition, we do not observe $\nu(\text{Ge-H})$ stretching modes for methylamine adsorption on Ge(100)-2 × 1.¹⁵

Either type of dissociation reaction is unexpected since Mui et al. found that all methylamines are trapped in the dative-bonded state on Ge(100)-2 × 1 at room temperature.¹⁵ In addition, we also observe very weak $\nu(\text{N-H})$ and $\nu(\text{CH}_2)$ stretching vibrations near 3223 and 2880 cm^{-1} , respectively, as well as $\delta(\text{CH}_2)$ deformation modes at 1454, 1367, and 1291 cm^{-1} . Although clearly visible in the multilayer near 1580 cm^{-1} , $\delta(\text{NH}_2)$ scissoring modes are not observed above the noise following the 0.5 L exposure of ethylenediamine (Figure 2a). While we cannot completely rule out a small quantity of undissociated amine at low coverage, the absence of $\delta(\text{NH}_2)$ scissoring modes suggests that the majority of amine groups undergo N–H dissociation at low coverage (Figure 1b).

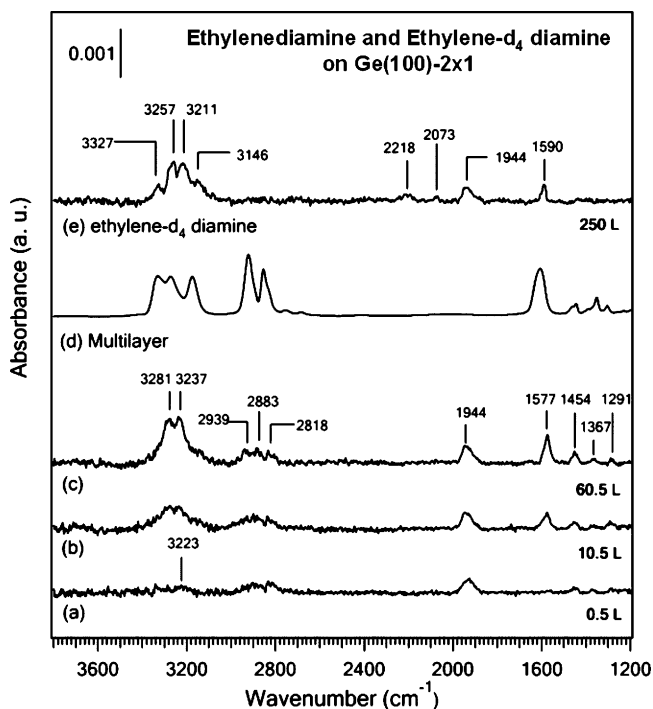


Figure 2. IR spectra of (a) 0.5, (b) 10.5, and (c) 60.5 L (saturation) ethylenediamine at 300 K, (d) ethylenediamine multilayer at 130 K, and (e) 250 L (saturation) ethylene- d_4 diamine at 300 K.

Although prior investigations report that N–H dissociation reactions are more likely than C–H dissociation on Si(100)-2 × 1 and Ge(100)-2 × 1,^{12–14,17,18} we can directly determine which reaction is occurring by employing ethylene- d_4 diamine, where the C–H bonds have been replaced by C–D bonds. If C–D dissociation is the majority pathway at low exposure, one would expect to observe $\nu(\text{Ge-D})$ stretches near 1420 cm^{-1} .³⁹ Figure 2e shows the IR spectrum of a 250 L ethylene- d_4 diamine saturation exposure on Ge(100)-2 × 1 at room temperature. For comparison, the 60.5 L exposure of ethylenediamine (Figure 2c) is also a saturation exposure. No $\nu(\text{Ge-D})$ modes are observed, and the $\nu(\text{Ge-H})$ peak at 1944 cm^{-1} is approximately the same intensity as that for ethylenediamine, indicating that N–H dissociation is the dominant reaction pathway. The retention of C–D bonds is confirmed by asymmetric and symmetric $\nu(\text{CD}_2)$ stretching modes at 2218 and 2073 cm^{-1} , respectively. Additionally, peaks associated with $\nu(\text{N-H})$ stretching modes are observed at 3327, 3257, 3211, and 3146 cm^{-1} . We attribute the differences in the $\nu(\text{N-H})$ stretching region for ethylenediamine (Figure 2c) and ethylene- d_4 diamine (Figure 2e), particularly the presence of new peaks at 3327 and 3146 cm^{-1} for ethylene- d_4 diamine, to shifts commonly observed for isotopically labeled compounds.^{21,40} Exposure of ethylenediamine- d_4 , where the N–H bonds have been replaced by N–D bonds, could be used to further verify the N–H dissociation reaction, however, this compound is currently not commercially available.

In Figure 3, the coverage-dependent IR data of Figure 2 are converted to difference spectra, where each spectrum is ratioed to the previous spectrum to show incremental changes. The difference spectra enable the identification of low and high coverage surface adducts. As the ethylenediamine exposure is increased from 0.5 to 10.5 L and then to 60.5 L, growth of the $\nu(\text{Ge-H})$ mode near 1950 cm^{-1} decreases while a strong $\delta(\text{NH}_2)$ scissoring deformation mode becomes clearly visible near 1577 cm^{-1} . In addition, $\nu(\text{N-H})$ stretching modes become more clearly resolved at 3283 and 3234 cm^{-1} . By the final

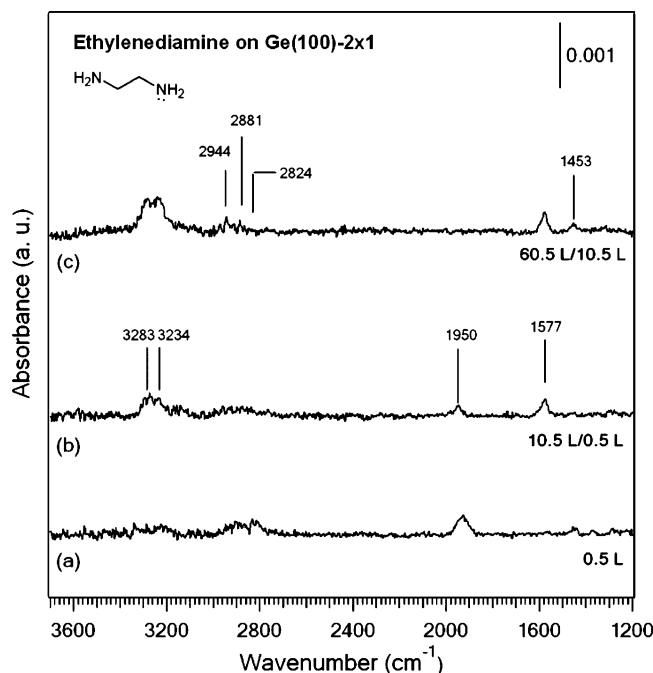


Figure 3. Incrementally ratioed IR spectra of ethylenediamine on Ge(100) at 300 K. Spectrum (a) is ratioed to the clean surface, and spectra (b) and (c) are ratioed to the indicated coverage.

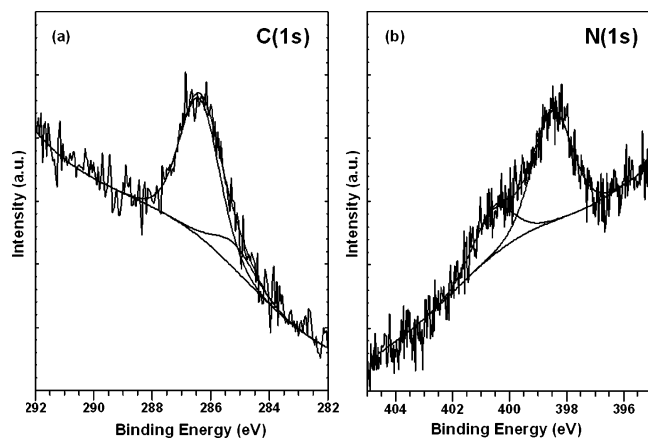


Figure 4. (a) C(1s) and (b) N(1s) photoelectron spectra of a 10 L saturation exposure of ethylenediamine on Ge(100)-2 \times 1 at room temperature. The fwhm of the C(1s) and N(1s) photoelectron components is 1.60 and 1.63 eV, respectively.

saturation exposure of 60.5 L (Figure 3c), the $\nu(\text{Ge-H})$ mode has already saturated while the $\nu(\text{NH}_2)$ and $\delta(\text{NH}_2)$ modes continue to exhibit growth. These data suggest that a different adsorption structure forms at higher surface coverages. The growth of $\nu(\text{N-H})$ stretching and $\delta(\text{NH}_2)$ scissoring modes, as well as the lack of $\nu(\text{Ge-H})$ stretching modes, indicates that the high-coverage surface structure is a molecularly adsorbed dative bond.

The X-ray photoelectron spectra shown in Figure 4 confirm the presence of a dative bond on the surface. Figure 4a shows the C(1s) photoelectron spectrum following a 10 L saturation exposure of ethylenediamine on Ge(100)-2 \times 1 at room temperature. Low coverage XPS spectra could not be collected due to prohibitively low signal-to-noise ratios. Due to the resolution of our dual anode X-ray source, only two components can be reasonably fit at 286.4 and 285.1 eV. While the location of the most intense peak agrees with previously reported values of various amines adsorbed on Si(100)-2 \times 1,^{13,31,41} it is difficult to glean any specific chemical information from this spectrum.

However, the N(1s) photoelectron spectrum shown in Figure 4b provides more information. Two components at 398.5 and 400.5 eV are visible in this spectrum. On the basis of previous studies of various methyl- and alkylamines adsorbed on Si(100)-2 \times 1,^{13,31} it is possible to assign the N(1s) components. Since the Pauling electronegativity difference between that of germanium (2.01) and nitrogen (3.0) is expected to increase the electron density at the nitrogen atom, the low binding energy peak is primarily attributed to the N-H dissociation product, that is, one in which nitrogen is covalently bonded to Ge. On the other hand, in the dative-bonded state, the nitrogen atom participating in the bond has donated its lone pair to the surface and an increase in the N(1s) binding energy would be expected. We therefore assign the high binding energy component to a dative-bonded nitrogen atom. The observed N(1s) binding energy shift between the N-H dissociated and dative-bonded products of ethylenediamine on Ge(100)-2 \times 1 is approximately 1.0 eV less than that for the case of amines on Si(100)-2 \times 1,^{13,31} suggesting that less charge is transferred to the surface in the dative-bonded state on Ge(100)-2 \times 1. Taken together, the two N(1s) peaks indicate a mixture of dissociative and dative-bonded products for ethylenediamine at saturation, in agreement with the IR data.⁴² While the intensity ratio of the two N(1s) photoelectron components is approximately 2.5:1, it is difficult to ascertain the product distribution because we cannot definitively determine whether a single or dual dative bond occurs at high coverage, a subject that we will now address.

Given the resolution of the IR and photoelectron data, it is difficult to determine whether the high-coverage dative-bonded surface product involves donation of one (intradimer, Figure 1a) or both (interdimer, Figure 1b) nitrogen lone pairs to the surface. On the basis of a simple coverage argument, the decrease in the number of adjacent, unreacted dimers at higher coverages would prevent interdimer reactions and a single dative bond would be more favorable. As will be discussed below, such a singly dative-bonded product may be blocked from N-H dissociation by a large activation barrier. Furthermore, estimates of coverage suggest some single dative bonds exist. A comparison of the entire C(1s) peak area with that of pyridine, which has five carbons and is reported to saturate at 0.25 ML on Ge(100)-2 \times 1,³³ enables us to determine that the saturation coverage of ethylenediamine is approximately 0.35 ML (0.25 ML = one molecule of ethylenediamine per two surface dimers), indicating that at least some ethylenediamine molecules must bond to a single dimer. On the other hand, if the high-coverage surface structure were predominantly a singly dative-bonded adduct (Figure 1a), where one amine group donates to the surface dimer and the other does not, two distinct $\delta(\text{NH}_2)$ scissoring peaks, arising from the free and dative-bonded amine groups, would be likely. For example, it has previously been observed that the $\delta(\text{NH}_2)$ scissoring mode of methylamine red shifts when molecularly adsorbed as a N-dative bond on Ge(100)-2 \times 1.¹⁵ However, Figures 2 and 3 both show a single, narrow absorption mode at 1577 cm^{-1} , indicating that both amine groups are in similar environments, suggesting a dual dative bond. The single $\delta(\text{NH}_2)$ scissoring peak for ethylenediamine is red shifted 20 cm^{-1} from its frequency in the multilayer and is thus consistent with the dual dative bond at high coverage. Changes in the electronic structure at the surface due to neighboring adsorbates, as reported for ammonia adsorption on Si(100)-2 \times 1,^{43,44} could account for the inhibition of the N-H dissociation reaction at higher coverage and appearance of intact, dual dative-bonded surface products. Further

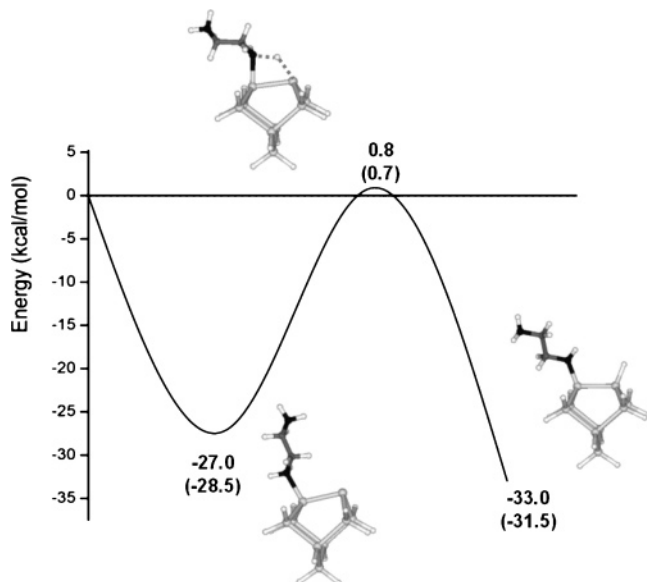


Figure 5. Calculated potential energy surface for the intradimer N–H dissociation of ethylenediamine on a Ge_9H_{12} single-dimer cluster. The values calculated for dimethylamine are included in parentheses for comparison.

experiments are necessary before a definitive conclusion can be reached as to which type of dative bond is present at high coverage, and STM studies are currently underway.

Our results differ substantially from those of Mui et al. where it was previously reported that simple methylamines form only Ge–N dative bonds on Ge(100)-2 × 1 at room temperature.¹⁵ The situation is more complex for the case of ethylenediamine due to the presence of a second amine group and ethylene spacer. Density functional theory provides a method with which to address questions of structure and its effect on reaction thermodynamics and kinetics. Table 1 shows calculated adsorption energies of ethylenediamine chemisorbed with the adsorption configurations illustrated in Figure 1. In agreement with our experimental observations at low surface exposure, a dual

TABLE 1: Calculated Adsorption Energies for Various Surface Products of Ethylenediamine on Ge(100)-2 × 1

	reaction	E_{ads} (kcal/mol)
single dimer	dative bond	–27.0
	N–H dissociation	–33.0
interdimer	dual dative bond	–43.7
	single dative bond/single N–H dissociation	–56.5
	dual N–H dissociation	–60.0

N–H dissociation reaction on neighboring dimers in adjacent rows is found to be the thermodynamically favored surface adduct on Ge(100)-2 × 1.

In addition to the calculated binding energies, which are consistent with our experimental observations, the calculated activation barriers are also supportive of the experimental results showing the dual N–H dissociation reaction. Figure 5 illustrates the potential energy surface for the pathway leading to the single-dimer N–H dissociation product. The activation energy for the N–H dissociation reaction is 0.8 kcal/mol above the energy of the reactants (27.8 kcal/mol above the dative-bonded state). As shown in Figure 5, the energetics of the single-dimer N–H dissociation pathway for ethylenediamine are nearly identical to those calculated for dimethylamine (shown in parentheses in Figure 5), a molecule which is not observed to dissociate on Ge(100)-2 × 1 at room temperature.¹⁵ Moreover, a recent theoretical study by Mui and Musgrave reports an additional 4.4 kcal/mol destabilization of the N–H dissociation transition state of ammonia on a larger, three-dimer Ge(100) cluster model.³² These findings therefore imply that another pathway leading to the dual N–H dissociated product is likely active for ethylenediamine on Ge(100)-2 × 1.

Another pathway leading to the experimentally observed N–H dissociation product involves two Ge dimers in adjacent rows, as shown in Figure 1b. Figure 6 illustrates the calculated critical points of this pathway. Initially, ethylenediamine adsorbs in a dual dative-bonded precursor state, where both amine lone pairs donate to the electrophilic dimer atoms of neighboring dimers, a state which lies 43.7 kcal/mol below the entrance

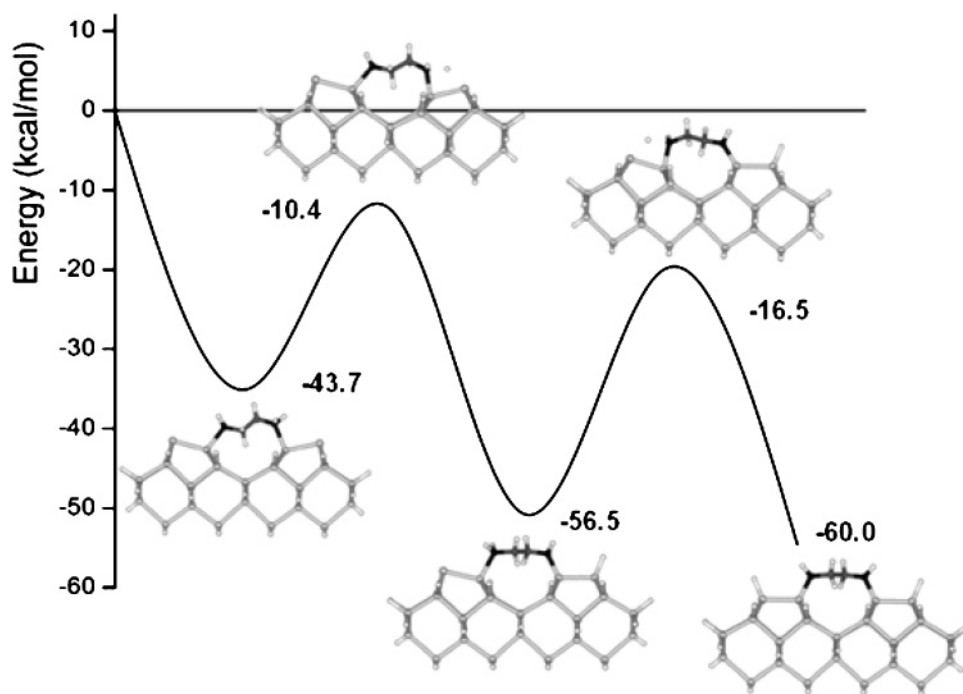


Figure 6. Calculated potential energy surface for the interdimer N–H dissociation of ethylenediamine on the $\text{Ge}_{31}\text{H}_{32}$ trench cluster.

channel. Although it is reasonable to expect that ethylenediamine will initially donate a single nitrogen lone pair to form a singly dative-bonded surface adduct, attempts to isolate such a product were unsuccessful because geometry optimizations, beginning with either a $c(4 \times 2)$ or a $p(2 \times 2)$ trench cluster, always led to a dual dative bond on a $c(4 \times 2)$ cluster. This theoretically observed dimer flipping upon the adsorption of ethylenediamine on a $p(2 \times 2)$ reconstruction indicates that adsorbate-induced dimer flipping has little or no barrier and is consistent with previous STM studies of nitrogen-containing aromatics on $\text{Ge}(100)\text{-}2 \times 1$.^{33,34}

From the dual dative bond, it is now possible for ethylenediamine to transfer a hydrogen atom to each surface dimer, thus creating a dual N–H dissociation product. The activation barriers for the transfer of the first and second hydrogen atom are -10.4 and -16.5 kcal/mol below the energy of the reactants, respectively. It is important to note that the absolute heights of each barrier from the dual dative bond and single N–H dissociated state are 33.3 and 40.0 kcal/mol, respectively. These are both larger than the 27.8 kcal/mol absolute barrier on a Ge_9H_{12} cluster for single N–H dissociation. However, if minimal thermal accommodation upon adsorption in the dual dative-bonded state is assumed, then the incident molecule may retain enough energy to surmount these barriers to N–H dissociation. Several previous reports indicate that reaction pathways where the activation energies lie below the entrance channel are often observed experimentally, even if they have large barriers from the fully accommodated precursor state.^{15,20} The increased stability of the dual dative bond (Figure 6) when compared to the single dative bond (Figure 5) leads to an N–H dissociation barrier substantially below the entrance channel and ultimately enables the experimental observation of the interdimer dual N–H dissociation product at room temperature.

Conclusions

We have investigated the surface reaction of ethylenediamine, a bifunctional molecule, on the $\text{Ge}(100)\text{-}2 \times 1$ surface at room temperature. In contrast to methylamines, the second amine functionality allows an interaction with neighboring surface dimers such that N–H dissociation is possible. At low coverage, the thermodynamically favored dual N–H dissociation dominates on $\text{Ge}(100)\text{-}2 \times 1$, while, at higher coverages, a dative-bonded product is more favorable, although its exact bonding configuration cannot be definitively determined from vibrational and photoelectron spectra alone.

Acknowledgment. A.K. would like to acknowledge financial support to carry out research at Stanford University from the Brain Korea 21 Project and the National R&D Project for Nano Science and Technology. Additionally, S.K. acknowledges financial support from KOSEF and the Center for Nanotubes and Nanostructured Composites and the Advanced Backbone IT Technology Development Project of the Ministry of Information and Communication. M.A.F. acknowledges support from the National Science Foundation in the form of a graduate research fellowship. S.F.B. acknowledges financial support from the National Science Foundation (CHE 0245260).

References and Notes

- (1) Lopinski, G. P.; Wayner, D. D. M.; Wolkow, R. A. *Nature* **2000**, *406*, 48.
- (2) Hurley, P.; Ribbe, A.; Buriak, J. J. *Am. Chem. Soc.* **2003**, *125*, 11334.
- (3) Guisinger, N. P.; Greene, M. E.; Basu, R.; Baluch, A. S.; Hersam, M. C. *Nano Lett.* **2004**, *4*, 55.
- (4) Bitzer, T.; Richardson, N. V. *Appl. Phys. Lett.* **1997**, *71*, 662.
- (5) Bitzer, T.; Richardson, N. V. *Appl. Surf. Sci.* **1999**, *145*, 339.
- (6) Kim, A.; Filler, M. A.; Kim, S.; Bent, S. F. *J. Am. Chem. Soc.* **2005**, *127*, 6123.
- (7) Wolkow, R. A. *Annu. Rev. Phys. Chem.* **1999**, *50*, 413.
- (8) Hamers, R. J.; Coulter, S. K.; Ellison, M. D.; Hovis, J. S.; Padowitz, D. F.; Schwartz, M. P.; Greenlief, C. M.; Russell, J. N. *Acc. Chem. Res.* **2000**, *33*, 617.
- (9) Bent, S. F. *Surf. Sci.* **2002**, *500*, 879.
- (10) Filler, M. A.; Bent, S. F. *Prog. Surf. Sci.* **2003**, *73*, 1.
- (11) Kubby, J. A.; Boland, J. J. *Surf. Sci. Rep.* **1996**, *26*, 61.
- (12) Cao, X.; Coulter, S. K.; Ellison, M. D.; Liu, H.; Liu, J.; Hamers, R. J. *J. Phys. Chem. B* **2001**, *105*, 3759.
- (13) Cao, X. P.; Hamers, R. J. *J. Am. Chem. Soc.* **2001**, *123*, 10988.
- (14) Mui, C.; Wang, G. T.; Bent, S. F.; Musgrave, C. B. *J. Chem. Phys.* **2001**, *114*, 10170.
- (15) Mui, C.; Han, J. H.; Wang, G. T.; Musgrave, C. B.; Bent, S. F. *J. Am. Chem. Soc.* **2002**, *124*, 4027.
- (16) Hossain, M. Z.; Machida, S.; Yamashita, Y.; Mukai, K.; Yoshinobu, J. *J. Am. Chem. Soc.* **2003**, *125*, 9252.
- (17) Carman, A. J.; Zhang, L. H.; Liswood, J. L.; Casey, S. M. *J. Phys. Chem. B* **2003**, *107*, 5491.
- (18) Wu, J. B.; Yang, Y. W.; Lin, Y. F.; Chiu, H. T. *J. Phys. Chem. B* **2004**, *108*, 1677.
- (19) Rangan, S.; Kubsy, S.; Gallet, J. J.; Bournel, F.; Le Guen, K.; Dufour, G.; Rochet, F.; Funke, R.; Knepe, M.; Piaszenski, G.; Kohler, U.; Sirotti, F. *Phys. Rev. B* **2005**, *71*, 125320.
- (20) Wang, G. T.; Mui, C.; Musgrave, C. B.; Bent, S. F. *J. Am. Chem. Soc.* **2002**, *124*, 8990.
- (21) Filler, M. A.; Van Deventer, J. A.; Keung, A. J.; Bent, S. F. *J. Am. Chem. Soc.* **2005**, submitted for publication.
- (22) Teague, L. C.; Boland, J. J. *J. Phys. Chem. B* **2003**, *107*, 3820.
- (23) Kim, A.; Choi, D. S.; Lee, J. Y.; Kim, S. *J. Phys. Chem. B* **2004**, *108*, 3256.
- (24) Zandvliet, H. J. W. *Phys. Rep.* **2003**, *388*, 1.
- (25) Shirley, D. A. *Phys. Rev. B* **1972**, *5*, 4709.
- (26) Kohn, W.; Sham, L. J. *Phys. Rev.* **1965**, *140*, A1133.
- (27) Hay, P. J.; Wadt, W. R. *J. Chem. Phys.* **1985**, *82*, 299.
- (28) Phillips, M. A.; Besley, N. A.; Gill, P. M. W.; Moriarty, P. *Phys. Rev. B* **2003**, *67*.
- (29) Ferrer, S.; Torrelles, X.; Etgens, V. H.; van der Vegt, H. A.; Fajardo, P. *Phys. Rev. Lett.* **1995**, *75*, 1771.
- (30) Widjaja, Y.; Musgrave, C. B. *Surf. Sci.* **2000**, *469*, 9.
- (31) Cao, X. P.; Hamers, R. J. *J. Vac. Sci. Technol., B* **2002**, *20*, 1614.
- (32) Mui, C.; Musgrave, C. B. *Langmuir* **2005**, *21*, 5230.
- (33) Kim, H. J.; Cho, J. H. *J. Chem. Phys.* **2004**, *120*, 8222.
- (34) Lee, J. Y.; Jung, S. J.; Hong, S.; Kim, S. *J. Phys. Chem. B* **2005**, *109*, 348.
- (35) Takagi, Y.; Yoshimoto, Y.; Nakatsuji, K.; Komori, F. *J. Phys. Soc. Jpn.* **2003**, *72*, 2425.
- (36) Takagi, Y.; Yoshimoto, Y.; Nakatsuji, K.; Komori, F. *Surf. Sci.* **2004**, *559*, 1.
- (37) Berg, R. W.; Rasmussen, K. *Spectrochim. Acta A* **1974**, *30*, 1881.
- (38) Borring, A.; Rasmussen, K. *Spectrochim. Acta A* **1975**, *31*, 889.
- (39) Chabal, Y. J. *Surf. Sci.* **1986**, *168*, 594.
- (40) Eng, J.; Raghavachari, K.; Struck, L. M.; Chabal, Y. J.; Bent, B. E.; Flynn, G. W.; Christman, S. B.; Chaban, E. E.; Williams, G. P.; Radermacher, K.; Manti, S. *J. Chem. Phys.* **1997**, *106*, 9889.
- (41) Ellison, M. D.; Hovis, J. S.; Liu, H. B.; Hamers, R. J. *J. Phys. Chem. B* **1998**, *102*, 8510.
- (42) To determine if the observed coverage dependence was actually a flux dependence, experiments were carried out at different pressures with a constant total exposure (not shown). However, exposure pressures ranging from 10^{-9} to 10^{-6} Torr revealed no significant differences in the C(1s) or N(1s) photoelectron spectra.
- (43) Queeney, K. T.; Chabal, Y. J.; Raghavachari, K. *Phys. Rev. Lett.* **2001**, *86*, 1046.
- (44) Widjaja, Y.; Musgrave, C. B. *J. Chem. Phys.* **2004**, *120*, 1555.